

Different Facets of Chaos in Quantum Mechanics

V.R. Manfredi⁽¹⁾ and L. Salasnich⁽²⁾

⁽¹⁾Dipartimento di Fisica “G. Galilei”, Università di Padova,
Istituto Nazionale di Fisica Nucleare, Sezione di Padova,
Via Marzolo 8, I-35131 Padova, Italy

⁽²⁾Istituto Nazionale per la Fisica della Materia, Unità di Milano,
Dipartimento di Fisica, Università di Milano,
Via Celoria 16, I-20133 Milano, Italy

Abstract

Nowadays there is no universally accepted definition of quantum chaos. In this paper we review and critically discuss different approaches to the subject, such as Quantum Chaology and the Random Matrix Theory. Then we analyze the problem of dynamical chaos and the time scales associated with chaos suppression in quantum mechanics.

PACS Numbers: 05.45.+b, 03.65.Bz

1 Introduction

The aim of this paper is to review and discuss various definitions and approaches to *quantum chaos*.^{1–5}

As yet, there is no universally accepted definition of quantum chaos. On the contrary, the meaning of classical chaos is beyond question. In classical mechanics a trajectory $\mathbf{z}(t)$ in the phase space Ω is chaotic if its maximal Lyapunov exponent λ is positive. The Lyapunov exponent is defined as

$$\lambda = \lim_{t \rightarrow \infty} \frac{1}{t} \ln |\omega(t)|, \quad (1)$$

where $\omega(t)$ is a tangent vector to $\mathbf{z}(t)$ with the condition that $|\omega(0)| = 1$. The exponential instability of chaotic trajectories implies a continuous frequency spectrum of motion. The continuous spectrum, in turn, implies correlation decay; this property, which is called *mixing* in ergodic theory, is the most important property of dynamical motion for the validity of the statistical description.^{6–8}

The problem of quantum chaos arose because the above mentioned condition of continuous spectrum for classical chaos is violated in quantum mechanics. Indeed the energy and the frequency spectrum of any quantum motion, bounded in phase space, are always discrete due to the non-commutative geometry (discreteness) of the phase space. According to the theory of dynamical systems, such motion corresponds to the limiting case of regular motion. It means that there is no classical-like chaos at all in quantum mechanics.^{1–5}

Nevertheless, we shall show that it is reasonable and useful to apply

the word *chaos* also in quantum mechanics. In the first part of this article some definitions of quantum chaos for stationary systems are discussed, while in the second part, the time evolution of classical and quantum systems is compared.

2 Quantum Chaology and Spectral Statistics

As is well known, in the study of the transition from order to chaos in classical systems a useful tool is the examination of the phase space properties, such as the Poincarè sections.⁶ Such plots are *not* directly available in the case of quantum systems. In many papers, the Berry definition of quantum chaos is adopted: "Quantum Chaology is the study of semiclassical, but not classical, behaviour characteristic of systems whose classical motion exhibits chaos".⁸

The idea, also suggested by authors like Percival and Gutzwiller,² is to connect the behaviour of the eigenvalues and eigenfunctions of a quantum system to the different structure of the phase space of the corresponding classical system in the regular and chaotic region.

In the context of quantum chaology, the spectral statistics of the energy levels are of great importance. Mehta defined: "A spectral statistic is a quantity which can be calculated from an observed sequence of levels alone, without other information and whose average value and variance are known from the theoretical model. A suitable statistic is one which is sensitive for the properties to be compared or distinguished and is insensitive for other details".⁹ In particular, it has been found that the spectral statistics of systems with underlying classical chaotic behaviour and time-reversal symmetry

agree with the predictions of the Gaussian Orthogonal Ensemble (GOE) of Random Matrix Theory (RMT),⁹ whereas quantum analogs of classically integrable systems display the characteristics of the Poisson statistics.¹⁻⁵ Note that if the chaotic system is without time-reversal symmetry then, instead of the GOE, it follows the predictions of the Gaussian Unitary Ensemble (GUE).

The most used spectral statistics of the energy levels are $P(s)$ and $\Delta_3(L)$. $P(s)$ is the distribution of nearest-neighbour spacings $s_i = (\tilde{E}_{i+1} - \tilde{E}_i)$ of the unfolded levels \tilde{E}_i . It is obtained by accumulating the number of spacings that lie within the bin $(s, s + \Delta s)$ and then normalizing $P(s)$ to unit. As shown by Berry,^{10,11} for quantum systems whose classical analogs are integrable, $P(s)$ is expected to follow the Poisson distribution

$$P(s) = \exp(-s) . \quad (2)$$

On the other hand, quantal analogs of chaotic systems exhibit the spectral properties of GOE with

$$P(s) = \frac{\pi}{2} s \exp\left(-\frac{\pi}{4} s^2\right) , \quad (3)$$

which is the so-called Wigner distribution. Note that for systems without time-reversal symmetry the GUE predicts $P(s) = (32/\pi^2) s^2 \exp(-4s^2/\pi)$.

The statistic $\Delta_3(L)$ is defined, for a fixed interval $(-L/2, L/2)$, as the least-square deviation of the staircase function $N(E)$ from the best straight line fitting it:

$$\Delta_3(L) = \frac{1}{L} \min_{A,B} \int_{-L/2}^{L/2} [N(E) - AE - B]^2 dE ,$$

where $N(E)$ is the number of levels between E and zero for positive energy, between $-E$ and zero for negative energy. The $\Delta_3(L)$ statistic provides a measure of the degree of rigidity of the spectrum: for a given interval L , the smaller $\Delta_3(L)$ is, the stronger is the rigidity, signifying the long-range correlations between levels. For this statistic the Poissonian prediction is

$$\Delta_3(L) = \frac{L}{15} . \quad (4)$$

The GOE predicts the same behaviour for $L \ll 1$; instead for $L \gg 1$ it gives

$$\Delta_3(L) = \frac{1}{\pi^2} \log L . \quad (5)$$

In the GUE case one has $\Delta_3(L) = (1/2\pi^2) \log L$. It is useful to remember that Berry¹² has shown that $\Delta_3(L)$ deviates from the universal predictions of RMT for very large L .

Another probe, which is generally regarded (see for instance Ref. 14) as very sensitive to the structure of chaotic states, is the transition probability. For reasons of space, we mention only the pioneering work of French and his coworkers¹³ and two more recent works concerning the interacting-boson model¹⁴ (IBM) and the three-level Lipkin, Meshkov, Glick (LMG) model.¹⁵ In both works the results based on the transition probabilities between eigenstates of the system completely agree with the spectral statistics $P(s)$ and $\Delta_3(L)$.

It is important to stress that even though the classical system is not known, to distinguish between ordered and chaotic states, the spectral statistics and the transition probabilities can be used.^{16–19}

3 From Poisson to GOE Transition: Comparison with Experimental Data

The agreement between the classical order-chaos transition and the quantal Poisson-GOE transition has been tested in many theoretical models, ranging from simple billiards^{20–22} to more realistic systems like nuclei^{23–26} and elementary particles.^{27–29}

In this section we shall compare the transition Poisson-GOE with the experimental data of two different systems: the atomic nuclei and the Hydrogen atom in a static magnetic field.

3.1 Atomic Nuclei

In atomic nuclei, as in other many-body systems, ordered and chaotic states generally coexist.¹⁷

a) The Low Energy Region

The behaviour of spectral statistics near the ground state has been studied by Garret, German, Courtney and Espino¹⁷ and Shriner, Mitchell and Von Egidy¹⁷. The main results of these authors have been shown in Figure 1 and Figure 2. As can be seen from the figures, in the low energy region the spectral statistics are in agreement with the Poisson ensemble or intermediate between Poisson and GOE.

b) The High Energy Region

Neutron resonance spectroscopy on a heavy even-even nucleus typically leads to the identification of about 150 to 170 s-wave resonances with $J^\pi = \frac{1}{2}^+$ located 8-10 MeV above the ground state of the compound system, with average spacings around 10 eV and average total widths around 1 eV. Proton resonance spectroscopy yields somewhat shorter sequences of levels with fixed spin and parity, with typically 60 to 80 members.

For the statistical analysis, it is essential that the sequences be pure (no admixture of levels with different spin or parity) and complete (no missing levels). Only such sequences were considered by Haq, Pandey and Bohigas.³⁰ Scaling each sequence to the same average level spacing and lumping together all sequences one leads to the "Nuclear Data Ensemble" (NDE), which contains 1726 level spacings.

As shown in Figure 3, the agreement between the experimental data and the GOE predictions is surprisingly good (in the GOE model there are no free parameters).

3.2 The Hydrogen Atom in the Strong Magnetic Field

We now discuss the local statistical properties of energy levels of a Hydrogen atom in a uniform strong magnetic field. The Hamiltonian of the system is given by

$$H = \frac{p^2}{2m} - \frac{e^2}{r} - \frac{qB}{2m}L_z + \frac{q^2B^2}{8m}(x^2 + y^2), \quad (6)$$

where the magnetic field B breaks the time-reversal symmetry. Although Eq. (6) is *not* time-reversal invariant, it can easily be written in a time-reversal invariant form.³¹ In fact, the paramagnetic interaction $\frac{qB}{2m}L_z$ simply shifts

the whole series of levels with a fixed quantum number M (eigenstate of L_z with eigenvalue $M\hbar$) and can be taken into account in the standard way: the Zeeman effect.

The Hamiltonian (6) written in atomic units $m = |q| = 4\pi\epsilon_0 = \hbar = 1$ is

$$H = \frac{p^2}{2} - \frac{1}{r} + \frac{\gamma^2}{8}(x^2 + y^2) , \quad (7)$$

where $\gamma = B/B_c$ is the magnetic field in atomic units and $B_c = 2.35 \cdot 10^5$ Tesla. This equation can be numerically solved for different values of the scaled energy $\epsilon = E/(2\gamma)^{2/3}$. Once the eigenvalues have been obtained, the spectral statistics $P(s)$ and $\Delta_3(L)$ can be calculated. Figure 4 shows the function $P(s)$ for different values of the scaled energy ϵ . Increasing ϵ , a smooth Poisson-GOE transition can be observed. Figure 5 shows the spectral rigidity $\Delta_3(L)$ in three different energy intervals. For this statistic the transition Poisson-GOE is also very clear.

In addition, a comparison has been made between the theoretical energy levels and the experimental ones; the agreement is excellent.

4 Quantum Chaos and Field Theory

In the last few years there has been much interest in chaos in field theories. It is now well known that the spatially uniform limits of scalar electrodynamics and Yang-Mills theory exhibit classical chaotic motion.³⁴ In this section we discuss quantum chaos in a field-theory schematic model, namely the spatially homogeneous SU(2) Yang-Mills-Higgs (YMH) system.^{27–29} The La-

grangian density of the SU(2) YMH system is given by

$$L = \frac{1}{2}(D_\mu\phi)^\dagger(D^\mu\phi) - V(\phi) - \frac{1}{4}F_{\mu\nu}^a F^{\mu\nu a}, \quad (8)$$

where

$$(D_\mu\phi) = \partial_\mu\phi - igA_\mu^b T^b\phi, \quad (9)$$

$$F_{\mu\nu}^a = \partial_\mu A_\nu^a - \partial_\nu A_\mu^a + g\epsilon^{abc} A_\mu^b A_\nu^c, \quad (10)$$

with $T^b = \sigma^b/2$, $b = 1, 2, 3$, generators of the SU(2) algebra, and where the potential of the scalar field (the Higgs field) is

$$V(\phi) = \mu^2|\phi|^2 + \lambda|\phi|^4. \quad (11)$$

In the (2+1)-dimensional Minkowski space ($\mu = 0, 1, 2$) and with spatially homogeneous Yang-Mills and the Higgs fields

$$\partial_i A_\mu^a = \partial_i\phi = 0, \quad i = 1, 2 \quad (12)$$

one considers the system in the region in which space fluctuations of fields are negligible compared to their time fluctuations.

In the gauge $A_0^a = 0$ and using the real triplet representation for the Higgs field one obtains

$$\begin{aligned} L = & \dot{\vec{\phi}}^2 + \frac{1}{2}(\dot{\vec{A}}_1^2 + \dot{\vec{A}}_2^2) - g^2[\frac{1}{2}\vec{A}_1^2\vec{A}_2^2 - \frac{1}{2}(\vec{A}_1 \cdot \vec{A}_2)^2 + \\ & + (\vec{A}_1^2 + \vec{A}_2^2)\vec{\phi}^2 - (\vec{A}_1 \cdot \vec{\phi})^2 - (\vec{A}_2 \cdot \vec{\phi})^2] - V(\vec{\phi}), \end{aligned} \quad (13)$$

where $\vec{\phi} = (\phi^1, \phi^2, \phi^3)$, $\vec{A}_1 = (A_1^1, A_1^2, A_1^3)$ and $\vec{A}_2 = (A_2^1, A_2^2, A_2^3)$.

When $\mu^2 > 0$, the potential V has a minimum at $|\vec{\phi}| = 0$, but for $\mu^2 < 0$ the minimum is at

$$|\vec{\phi}_0| = \sqrt{\frac{-\mu^2}{4\lambda}} = v,$$

which is the non zero Higgs vacuum. This vacuum is degenerate, and after spontaneous symmetry breaking the physical vacuum can be chosen $\vec{\phi}_0 = (0, 0, v)$. If $A_1^1 = q_1$, $A_2^2 = q_2$ and the other components of the Yang-Mills fields are zero, in the Higgs vacuum the Hamiltonian of the system reads

$$H = \frac{1}{2}(p_1^2 + p_2^2) + g^2 v^2 (q_1^2 + q_2^2) + \frac{1}{2} g^2 q_1^2 q_2^2, \quad (14)$$

where $p_1 = \dot{q}_1$ and $p_2 = \dot{q}_2$. Here $w^2 = 2g^2 v^2$ is the mass term of the Yang-Mills fields. This YMH Hamiltonian is a toy model for classical non-linear dynamics, with the attractive feature that the model emerges from particle physics. At low energy the motion near the minimum of the potential

$$V(q_1, q_2) = g^2 v^2 (q_1^2 + q_2^2) + \frac{1}{2} g^2 q_1^2 q_2^2, \quad (15)$$

where the Gaussian curvature is positive, is periodic or quasiperiodic and is separated from the instability region by a line of zero curvature; if the energy is increased, the system will be for some initial conditions in a region of negative curvature, where the motion is chaotic. According to this scenario, the energy E_c of chaos-order transition is equal to the minimum value of the line of zero Gaussian curvature $K(q_1, q_2)$ on the potential-energy surface. It is easy to show that the minimal energy on the zero-curvature line is given by:

$$E_c = V_{min}(K = 0, \bar{q}_1) = 6g^2 v^4, \quad (16)$$

and by inverting this equation one obtains $v_c = (E/6g^2)^{1/4}$. There is an order-chaos transition by increasing the energy E of the system and a chaos-order transition by increasing the value v of the Higgs field in the vacuum. Thus, there is only one transition regulated by the sole parameter $E/(g^2 v^4)$.

It is important to point out that *in general* the curvature criterion guarantees only a *local instability*¹⁶⁾ and should therefore be combined with the Poincarè sections¹⁷⁾. Chaotic regions on the surface of the section are characterized by a set of randomly distributed points, and regular regions by dotted or solid curves. Figure 6 shows the Poincarè sections, which confirm the analytical predictions of the curvature criterion: the critical value of the onset of chaos is in very good agreement with the Poincarè sections.

In quantum mechanics the generalized coordinates of the YMH system satisfy the usual commutation rules $[\hat{q}_k, \hat{p}_l] = i\delta_{kl}$, with $k, l = 1, 2$. Introducing the creation and destruction operators

$$\hat{a}_k = \sqrt{\frac{\omega}{2}}\hat{q}_k + i\sqrt{\frac{1}{2\omega}}\hat{p}_k, \quad \hat{a}_k^+ = \sqrt{\frac{\omega}{2}}\hat{q}_k - i\sqrt{\frac{1}{2\omega}}\hat{p}_k, \quad (17)$$

the quantum YMH Hamiltonian can be written

$$\hat{H} = \hat{H}_0 + \frac{1}{2}g^2\hat{V}, \quad (18)$$

where

$$\hat{H}_0 = \omega(\hat{a}_1^+\hat{a}_1 + \hat{a}_2^+\hat{a}_2 + 1), \quad (19)$$

$$\hat{V} = \frac{1}{4\omega^2}(\hat{a}_1 + \hat{a}_1^+)^2(\hat{a}_2 + \hat{a}_2^+)^2, \quad (20)$$

with $\omega^2 = 2g^2v^2$ and $[\hat{a}_k, \hat{a}_l^+] = \delta_{kl}$, $k, l = 1, 2$. If $|n_1 n_2\rangle$ is the basis of the occupation numbers of the two harmonic oscillators, the matrix elements are

$$\langle n_1' n_2' | \hat{H}_0 | n_1 n_2 \rangle = \omega(n_1 + n_2 + 1)\delta_{n_1' n_1}\delta_{n_2' n_2}, \quad (21)$$

and

$$\langle n_1' n_2' | \hat{V} | n_1 n_2 \rangle = \frac{1}{4\omega^2}[\sqrt{n_1(n_1 - 1)}\delta_{n_1' n_1 - 2} + \sqrt{(n_1 + 1)(n_1 + 2)}\delta_{n_1' n_1 + 2} + (2n_1 + 1)\delta_{n_1' n_1}] \times$$

$$\times [\sqrt{n_2(n_2 - 1)}\delta'_{n_2 n_2 - 2} + \sqrt{(n_2 + 1)(n_2 + 2)}\delta'_{n_2 n_2 + 2} + (2n_2 + 1)\delta'_{n_2 n_2}] . \quad (22)$$

Figure 7 shows the $P(s)$ distribution for different values of the parameter v . The figure shows a Wigner-Poisson transition by increasing the value v of the Higgs field in the vacuum. The $P(s)$ distribution is fitted by the Brody function

$$P(s, \omega) = \alpha(\omega + 1)s^\omega \exp(-\alpha s^{\omega+1}) , \quad (23)$$

with

$$\alpha = (\Gamma[\frac{\omega + 2}{\omega + 1}])^{\omega+1} . \quad (24)$$

This function interpolates between the Poisson distribution ($\omega = 0$) of integrable systems and the Wigner distribution ($\omega = 1$) of chaotic ones, and thus the parameter ω can be used as a simple quantitative measure of the degree of chaoticity. By using the $P(s)$ distribution and the Brody function it is possible to give a quantitative measure of the degree of quantal chaoticity of the system. The numerical calculations of Figure 6 and 7 clearly show the quantum chaos-order transition and its connection to the classical one.

5 Alternative Approaches to Quantum Chaos

A different approach to quantum chaos has been discussed by Sakata and his coworkers.³⁵ The example discussed by Sakata is a system of an even number of fermions transformed into a boson system by means of the boson expansion theory,³⁶ where the boson system is described by K-kinds of boson operators $(B_j, B_j^+; j=1, \dots, K)$.

The main idea of Sakata³⁵ is that, just as in the classical theory a dissolution of integrability (with the KAM mechanism) simply means the onset of chaotic motion,^{7,8} in quantum systems a dissolution of quantum numbers may indicate the onset of quantum chaos. In accordance with the above definition of quantum chaos, we may classify the eigenstates $|i\rangle$ of the many-body Hamiltonian into three characteristic cases with the aid of the (μ, ν) -basis states, defined as $|\mu, \nu\rangle = |\mu_1 \dots \mu_L, \nu_{L+1} \dots \nu_K\rangle$, which are specified by K -kinds of quantum numbers.

- 1) Quantum integrable states: If one finds one of the $|\mu, \nu\rangle$ -basis states for a given eigenstate $|i\rangle$ satisfying $|\langle \mu, \nu | i \rangle|^2 = 1$, then $|i\rangle$ is classified as a *quantum integrable state*, see Figure 8(a).
- 2) Quantum KAM states: If $|i\rangle$ is described perturbatively starting from the $|\mu, \nu\rangle$ -basis state, then it is a *quantum KAM state*, see Figure 8(b).
- 3) Quantum chaotic states: If $|i\rangle$ is *not* described perturbatively starting from the $|\mu, \nu\rangle$ -basis state, then it is regarded as a *quantum chaotic state*, see Figure 8(c).

For further discussion of Sakata's approach see Ref. 35 and references quoted therein.

Recently, another approach to the order-chaos transition has been proposed by Soloviev in the framework of nuclear structure.^{37,38} Soloviev's main idea was to discuss the order to chaos transition in terms of the properties of nuclear wave-functions and to analyze how the structure of nuclear states changes with increasing excitation energy. He focused his attention on non-rotational states of rigid nuclei. The main conclusions are the following:

- 1) Order is governed by the large components of the wave function of the

excited states.

2) Chaos takes place in the small components of the wave function of the nuclear excited states. The excited states are chaotic if their wave functions are composed of only small components of many-quasiparticle or many-phonon configurations.

In our opinion these two approaches are quite similar and the Sakata approach also gives a simpler picture of the three cases discussed (regular, KAM, chaotic).

6 Dynamical Quantum Chaos and Time Scales

In this section we analyze in more detail the previously discussed problems of the chaotic time evolution for a quantum system.

A quantum system evolves according to a linear equation and this is an important feature which makes it different from a classical system, for which the equations of motion can be nonlinear. On the other hand, the Liouville equation of the density function is linear both in classical and quantum mechanics but the evolution operator of Liouville has different spectral properties. The classical Liouville operator has a continuous spectrum and this implies and allows chaotic motion. Instead, for bound systems, the quantum Liouville operator has a purely discrete spectrum, therefore no long-term chaotic behaviour.^{4,5}

As shown by Casati, Chirikov and coworkers^{39,40} studying toy models like the kicked rotor, the time evolution of a quantum state follows the classical one, including the chaotic phenomena, up to a *break time* t_B . After that, in

contrast to classical dynamics, we get localization (dynamical localization). This means that persistent chaotic behaviour in the evolution of the quantum states and observables is not possible. Roughly speaking, chaotic behaviour is possible in quantum mechanics only as a transient with lifetime t_B . The phenomenon of localization is clearly illustrated in Figure 9. This plot shows, in the case of the so-called standard map, the classical (solid curve) and quantum (dotted curve) unperturbed energy as a function of τ (number of map interactions).

The value of the break time t_B depends on the model studied and its exact behaviour is still controversial, but can be estimated from the Heisenberg indetermination principle as

$$t_B \simeq \frac{\hbar}{\Delta E} , \quad (25)$$

where ΔE is the mean spacing of energy levels. The discrete spectrum of the Liouville operator cannot be resolved if $t < t_B$, i.e. t_B is the time at which the quantal evolution (of a wave packet, for example) "realizes" that the spectrum of the evolution operator is discrete. According to the Thomas-Fermi rule, $\Delta E \propto \hbar^N$, where N is the number of degrees of freedom, i.e. the dimension of the configuration space. So, as $\hbar \rightarrow 0$, the break time diverges as $t_B \sim \hbar^{1-N}$, and it does so faster, the higher N is.

In the case of classical chaos, another time scale, *the random time scale* t_R , much shorter than t_B , can be introduced to estimate the time at which classical exponential spreading reaches the quantal resolution of the phase space. Thus, it is the full time for the exponential spreading of the minimum initial wave packet. As shown by Berman and Zaslavski⁴¹ the random time

(called the breaking time by the two authors) follows the logarithmic law

$$t_R \simeq \lambda^{-1} \ln \left(\frac{S}{\hbar} \right) , \quad (26)$$

where S is a classical action and λ is the Lyapunov exponent of the system. In particular, Berman and Zaslavski have studied two different models, which allow one to calculate the random time scale t_R . The first model is a periodically kicked oscillator, which gives $t_R = \ln(cost/\hbar)$. The second is an ensemble of N atoms interacting with light in the resonant cavity. For this model $t_R = \ln(cost N)$.

6.1 Mean-Field Approximation and Dynamical Chaos

Let us consider a N -body quantum system with Hamiltonian \hat{H} . The exact time-dependent Schrödinger equation can be obtained by imposing the quantum last action principle on the Dirac action

$$S = \int dt \langle \psi(t) | i\hbar \frac{\partial}{\partial t} - \hat{H} | \psi(t) \rangle , \quad (27)$$

where ψ is the many-body wavefunction of the system.⁴² Looking for stationary points of S with respect to variation of the conjugate wavefunction ψ^* gives

$$i\hbar \frac{\partial}{\partial t} \psi = \hat{H} \psi . \quad (28)$$

As is well known, it is usually impossible to obtain the exact solution of the many-body Schrödinger equation and some approximation must be used. In the mean-field approximation the total wavefunction is assumed to be composed of independent particles, i.e. it can be written as a product of

single-particle wavefunctions ϕ_j . In the case of identical fermions, ψ must be antisymmetrized. By looking for stationary action with respect to variation of a particular single-particle conjugate wavefunction ϕ_j^* one finds a time-dependent Hartree-Fock equation for each ϕ_j :

$$i\hbar \frac{\partial}{\partial t} \phi_j = \frac{\delta}{\delta \phi_j^*} \langle \psi | \hat{H} | \psi \rangle = \hat{h} \phi_j , \quad (29)$$

where \hat{h} is a one-body operator.⁴² The main point is that, in general, the one-body operator \hat{h} is nonlinear. Thus the Hartree-Fock equations are non-linear (integro-)differential equations. These equations can give rise, in some cases, to chaotic behaviour (dynamical chaos) of the mean-field wavefunction.

In the mean-field approximation the mathematical origin of *dynamical chaos* resides in the nonlinearity of the Hartree-Fock equations. These equations provide an approximate description, the best independent-particle description, which describes, for a certain time interval, the very complicated evolution of the true many-body system. Two questions then arise:

- 1) Does this chaotic behavior persist in time?
- 2) What is the best physical situation to observe this kind of nonlinearity?

To answer the first question, it should be stressed that, as shown previously, quantum systems evolve according to a linear equation. Since the Schrödinger equation is linear, so is any of its projections. Its time evolution follows the classical one, including chaotic behaviour, up to the break time t_B . After that, in contrast to the classical dynamics, we get dynamical localization. This means that persistent chaotic behaviour in the evolution of the states and observables is not possible. Nevertheless, we have seen that $t_B \sim \hbar^{1-N}$, where N is the number of degrees of freedom of the system, thus

for a large number of particles the break time can be very long.

Concerning the second question, it is useful to remember that, in the thermodynamic limit, i.e. when the number N of particles tends to infinity at constant density, the energy spectrum of the system is, in general, continuous and true chaotic phenomena are not excluded.⁴³

When the mean-field theory is a good approximation of the exact many-body problem, one can use the nonlinear mean-field equations to estimate the transient chaotic behaviour of the many-body system. An important case where such an approach could be applied is the Bose–Einstein condensate of weakly-interacting alkali-metal atoms.⁴⁴ In particular, we suggest that the collective oscillations of the Bose condensate^{45,46} can give rise to dynamical chaos.

7 Conclusions

In this paper we have reviewed various definitions of quantum chaos. In our opinion the simplest and clearest approach is that of Quantum Chaology, i.e. the study of quantum systems which are classically chaotic. Obviously, Quantum Chaology has some limitations, mainly it excludes systems without a classical analog, but its predictions in connection to the Random Matrix Theory are very accurate.

Nowadays there are at least two important problems under investigation: the study of chaos without classical analog and the transient chaoticity of quantum systems. The problem of chaos in systems without a clear classical analog is very intricate and new ideas, like those of Sakata and Soloviev

discussed here, are needed. Also the precise behaviour of the time scales of dynamical chaos in quantum systems is not fully understood but some remarks can be made.

We observe that the limitation to persistent chaotic dynamics in quantum systems does not apply if the spectrum of the Hamiltonian operator \hat{H} is continuous. In the thermodynamic limit, i.e. when the number N of particles tends to infinity at constant density, the spectrum is, in general, continuous and true chaotic phenomena are not excluded. We have seen that the break time t_B is very long for systems with many particles. The *transient chaotic dynamics* of quantum states and observables can be experimentally observed in many-body quantum systems. Moreover, the fact that the break time t_B increases with the number of microscopic degrees of freedom explains the chaotic behaviour of macroscopic systems, without invoking a role for the observer or the environment.

The study of quantum chaos for many-body or continuum systems (field theory) is a very promising field of research which can also help to better understand the foundations of quantum theory and statistical mechanics.

* * *

One of us (L.S.) is greatly indebted to Prof. M. Robnik for many suggestions.

References

1. O. de Almeida, *Hamiltonian Systems: Chaos and Quantization* (Cambridge University Press, Cambridge, 1988).
2. M.C. Gutzwiller, *Chaos in Classical and Quantum Mechanics* (Springer-Verlag, New York, 1990).
3. *Quantum Chaos*, Ed. by H.A. Cerdeira, R. Ramaswamy, M.C. Gutzwiller and G. Casati (World Scientific, Singapore, 1991); *From Classical to Quantum Chaos*, Conference Proceeding SIF **41**, Ed. by G.F. Dell'Antonio, S. Fantoni and V.R. Manfredi (Editrice Compositori, Bologna, 1993).
4. *Quantum Chaos*, Proc. of the Int. School "E. Fermi", Course CXIX, Ed. by G. Casati, I. Guarneri and U. Smilansky (North Holland, Amsterdam, 1993).
5. *Quantum Chaos*, Ed. by G. Casati and B. Chirikov (Cambridge Univ. Press, Cambridge, 1995).
6. H. Poincaré, *Les Methodes Nouvelles de la Mechanique Celeste* (Gauthier-Villars, Paris, 1892).
7. A.J. Lichtenberg and M.A. Lieberman, *Regular and Stochastic Motion*, (Springer-Verlag, New York, 1983).
8. M.V. Berry, in *Dynamical Chaos* (The Royal Society, London, 1987).
9. M.L. Mehta, in *Statistical Properties of Nuclei*, Ed. by J.B. Garg (1972); M.L. Mehta, *Random Matrices*, 2nd edition (Academic Press, 1991).
10. M.V. Berry and M. Tabor, Proc. Roy. Soc. A **356**, 375 (1977).
11. M.V. Berry, Ann. Phys. **131**, 163 (1981).
12. M.V. Berry, Proc. Roy. Soc. A **400**, 229 (1985).

13. T.A. Brody, J. Flores, J.B. French, P.A. Mello, A. Pandey and S.S.M. Wong, Rev. Mod. Phys. **53**, 385 (1981).
14. Y. Alhassid, A. Novoselsky and N. Whelan, Phys. Rev. Lett. **65**, 2971 (1990).
15. M.T. Lopez-Arias and V.R. Manfredi, Nuovo Cim. A **104**, 283 (1991).
16. P. Castiglione, G. Jona-Lasinio and C. Presilla, J. Phys. A: Math. Gen. **29**, 6169 (1996).
17. M.T. Lopez-Arias, V.R. Manfredi and L. Salasnich, La Rivista del Nuovo Cimento **17**, n. 5 (1994); J.D. Garrett, J.R. German, L. Courtney and J.M. Espino, in *Future Directions in Nuclear Physics*, Ed. by J. Dudek and B. Hass, American Institute of Physics (1992); J.F. Shriner, G.E. Mitchell and T. von Egidy, Z. Phys. A **338**, 309 (1990).
18. E. Caurier, J.M.G. Gomez, V.R. Manfredi and L. Salasnich, Phys. Lett. B **365**, 7 (1996).
19. J.M.G. Gomez, V.R. Manfredi, L. Salasnich and E. Caurier, Phys. Rev. C **58**, 2108 (1998).
20. O. Bohigas, M.J. Giannoni and C. Schmit, Phys. Rev. Lett. **52**, 1 (1984).
21. M.V. Berry and M. Robnik, J. Phys. A **19**, 649 (1986).
22. M.V. Berry and M. Robnik, J. Phys. A **20**, 2389 (1987).
23. V.R. Manfredi and L. Salasnich, Z. Phys. A **343**, 1 (1992).
24. V.R. Manfredi, L. Salasnich and L. Demattè, Phys. Rev. E **47**, 4556 (1993).
25. V.R. Manfredi and L. Salasnich, Int. J. Mod. Phys. E **4**, 625 (1995).
26. V.R. Manfredi, M. Rosa-Clot, L. Salasnich and S. Taddei, Int. J. Mod.

- Phys E **5**, 519 (1995).
27. L. Salasnich, Phys. Rev. D **52**, 6189 (1995).
 28. L. Salasnich, Mod. Phys. Lett. A **12**, 1473 (1997).
 29. L. Salasnich, Phys. Atom. Nucl. **61**, 1878 (1998).
 30. R. Haq, A. Pandey and O. Bohigas, Phys. Rev. Lett. **48**, 1086 (1982).
 31. D. Delande, in *Chaos and Quantum Physics*, Ed. by M.J. Giannoni, A. Voros, J. Zinn-Justin (North Holland, Amsterdam, 1991).
 32. H. Ruder, G. Wunner, H. Herold and F. Geyer, *Atoms in Strong Magnetic Fields* (Springer-Verlag, Berlin, 1994).
 33. J. Main, G. Wiebusch and K.H. Welge, in *Irregular Atomic Systems and Quantum Chaos*, Ed. by J.C. Gay (Gordon and Breach Science Publishers, New York, 1992).
 34. T.S. Birò, S.G. Matinyan and B. Müller, *Chaos and Gauge Field Theory* (World Scientific, Singapore, 1994).
 35. F. Sakata et al., Nucl. Phys. A **519**, 93c (1990).
 36. P. Ring and P. Schuck, *The Nuclear Many-Body Problem* (Springer-Verlag, Berlin, 1980).
 37. V.G. Soloviev, Nucl. Phys. A **554**, 77 (1993).
 38. V.G. Soloviev, Nucl. Phys. A **586**, 265 (1995).
 39. G. Casati, B.V. Chirikov, J. Ford and F.M. Izrailev, Lecture Notes in Physics. **93**, 334 (1979).
 40. C. Casati, J. Ford, I. Guarneri and F. Vivaldi, Phys. Rev. A **34**, 1413 (1986).
 41. G.P. Berman and G.M. Zaslavsky, Physica A **91**, 450 (1978).
 42. A. Fetter and J. Walecka, *Quantum Theory of Many Particle Systems*

(McGraw-Hill, New York, 1971).

43. G. Jona-Lasinio, C. Presilla and F. Capasso, Phys. Rev. Lett. **68**, 2269 (1992); G. Jona-Lasinio and C. Presilla, Phys. Rev. Lett. **77**, 4322 (1996).

44. M. H. Anderson *et al.*, Science **269**, 198 (1995); C. C. Bradley *et al.*, Phys. Rev. Lett. **75**, 1687 (1995); K. B. Davis *et al.*, Phys. Rev. Lett. **75**, 3969 (1995).

45. L. Reatto, A. Parola and L. Salasnich, J. Low Temp. Phys. **113**, 195 (1998).

46. E. Cerboneschi, R. Mannella, E. Arimondo and L. Salasnich, Phys. Lett. A **249**, 245 (1998).

Figure Captions

Figure 1: $P(s)$ for "cold" deformed rare-earth nuclei (adapted from Ref. 17).

Figure 2: Spectral statistics for nuclei with atomic mass $24 < A < 244$ and excitation energy of few MeV. a) $2+$ and 4^+ states, even-even nuclei; b) all other states, even-even nuclei; c) states with non-natural parity, odd-odd nuclei; d) states with natural parity, odd nuclei (adapted from Ref. 17).

Figure 3: Comparison of the nearest-neighbour spacing distribution $P(s)$ and spectral rigidity $\Delta_3(L)$ of the Nuclear Data Ensemble (NDE) with the GOE predictions (adapted from Ref. 30).

Figure 4: Histograms of the level distances of quantum energies in the Hydrogen atom in magnetic fields at different values of the scaled energy. The smooth curves are the results of the fits to the histograms (adapted from Ref. 32).

Figure 5: Spectral rigidity $\Delta_3(L)$ for energy level sequences of the Hydrogen atom in a magnetic field of 6 Tesla in three different energy intervals. The transition to the GOE distribution as soon as the classical motion becomes chaotic is also visible here (adapted from Ref. 32).

Figure 6: The Poincarè sections of the model. From the top: $v = 1$, $v = 1.1$ and $v = 1.2$. Energy $E = 10$ and interaction $g = 1$ (adapted from Ref. 28).

Figure 7: $P(s)$ distribution. From the top: $v = 1$ ($\omega = 0.92$), $v = 1.1$ ($\omega = 0.34$) and $v = 1.2$ ($\omega = 0.01$), where ω is the Brody parameter. First 100 energy levels and interaction $g = 1$. The dotted, dashed and solid curves stand for Wigner, Poisson and Brody distributions, respectively (adapted

from Ref. 28).

Figure 8: Exact eigenstates $|i\rangle$ expressed in the $|\mu, \nu\rangle$ basis states: a) Quantum Integrable States; b) Quantum KAM States; c) Quantum Chaotic States (adapted from Ref. 35).

Figure 9: Classical (solid curve) and quantum (dotted curve) unperturbed energy $\langle n^2(\tau) \rangle = 2E$ as a function of time τ (number of map iterations) (adapted from Ref. 5).

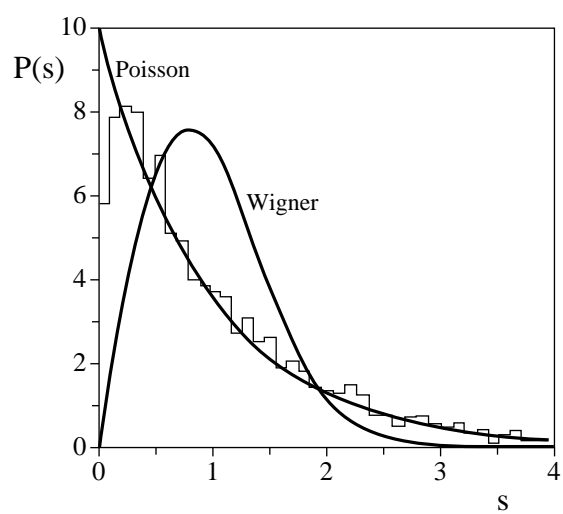


FIGURA 1

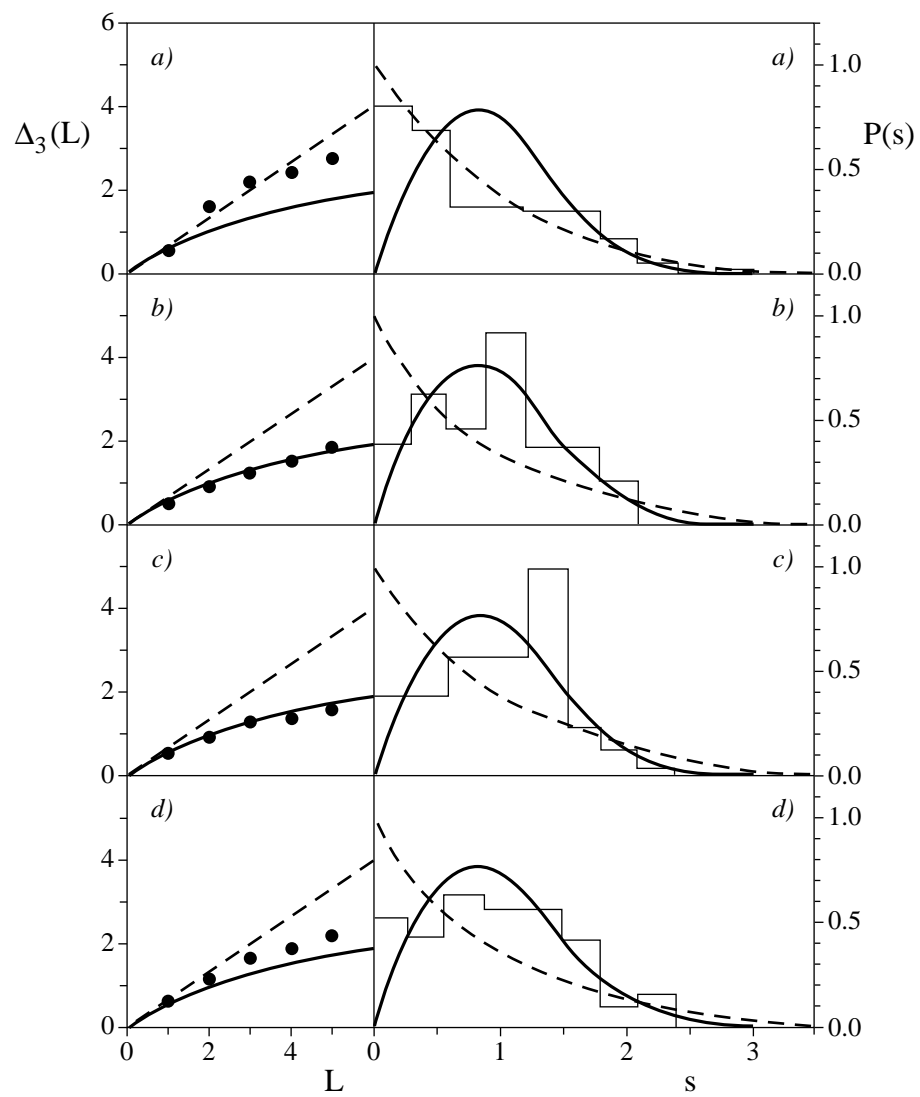


FIGURA 2

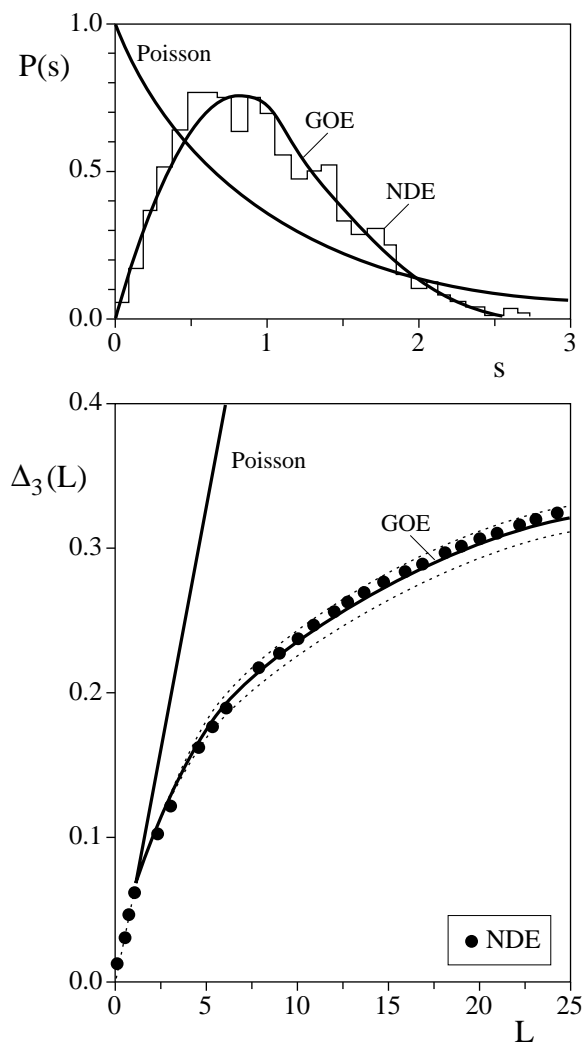


FIGURA 3

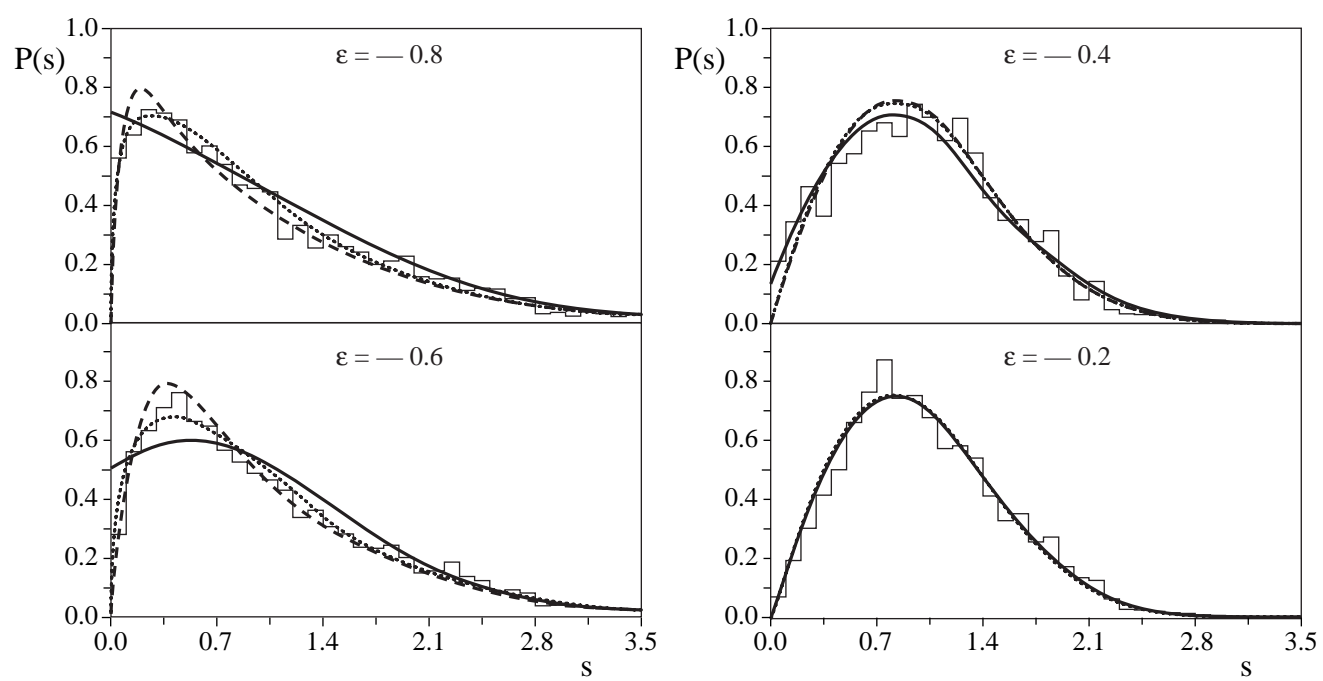


FIGURA 4

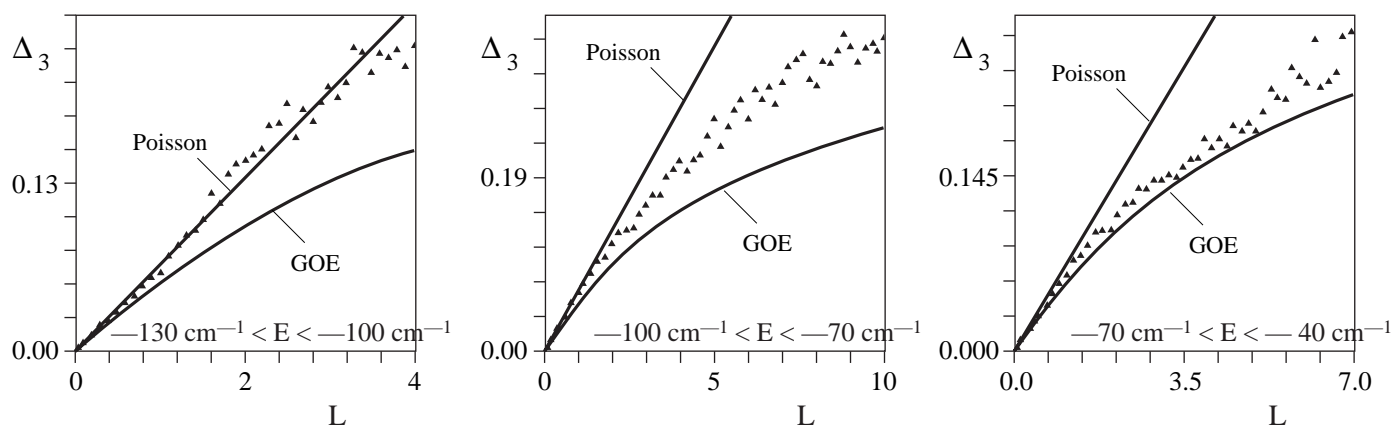


FIGURA 5

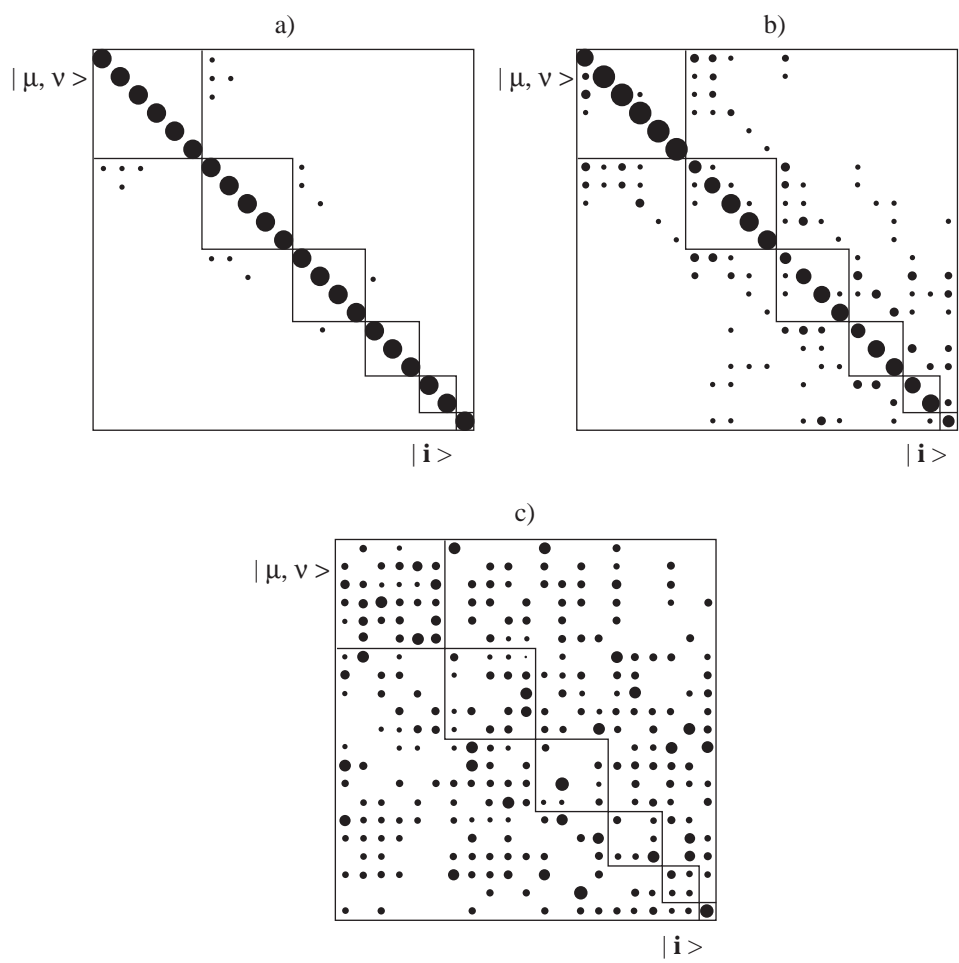


FIGURA 8

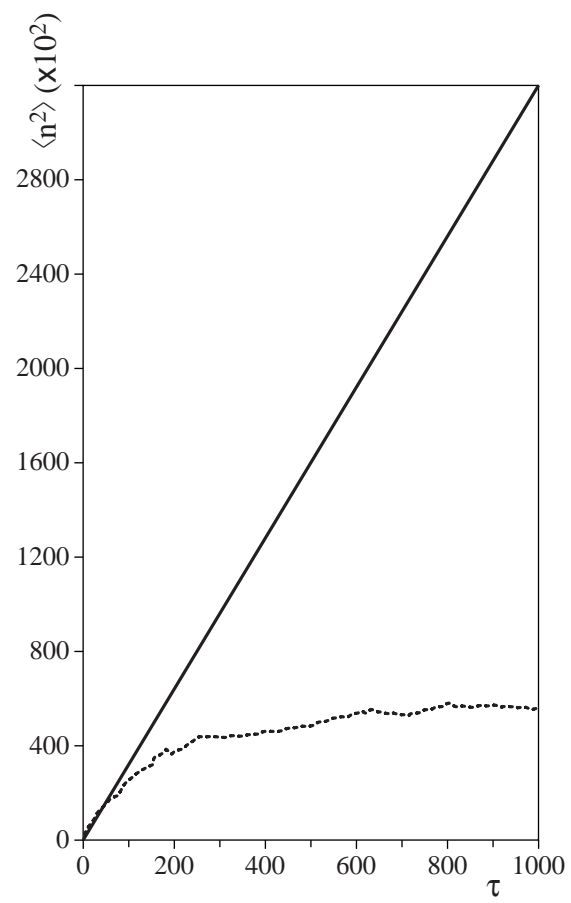


FIGURA 9